文章编号：1001-9014(2024)06-0820-07

DOI:10.11972/j.issn.1001-9014.2024.06.013

Research on power improvement of a LD directly-pumped mid-infrared pulse solid-state laser

ZHANG Meng[1], YANG Xi[1], GUO Jia-Wei[1], CAI He[1], WU Xin-Yang[2,1], HAN Ju-Hong[1], WANG Shun-Yan[1], WANG You[1*]

(1. Southwest Institute of Technical Physics, Chengdu 610083, China;
2. School of Materials Science and Engineering, Xinjiang University, Urumqi, 830046, China)

Abstract: An LD directly-pumped solid-state laser is considered to be one of the most promising mid-infrared light sources because of its simple principle, small size, and compact structure for the generation of mid-infrared (MIR) lasers in the 3-5 μm band. However, the quantum defect of LD directly-pumped MIR solid-state lasers will be much larger than that of ordinary near-infrared LD pumped solid-state lasers, which may lead to thermal damage and limit their development. In order to solve this problem, the methods of reducing the specific surface area of the crystal and improving the thermal energy released by the crystal structure are discussed, and the optimal length of the laser crystal is determined. The cooling structures of barium yttrium fluoride laser crystals (Ho^{3+}:BY_2F_8) of different lengths were studied by thermal simulation using COMSOL software. The experimental results show that the output power can be increased and the thermal stress in the laser crystal can be alleviated by using the laser crystal whose length is slightly shorter than that of the cooler. The final experiment shows that when the pump repetition rate is 15 Hz and the pulse width is 90 μs, the single pulse energy is 7.28 mJ at the output wavelength of 3.9 μm, which is about 3 times as large as that of the crystal with the length of 10 mm (2.81 mJ). Such results should be another breakthrough of our team since the first directly-pumped solid-state MIR laser was realized more than a year ago. It might pave the way for the construction of a feasible MIR laser in the near future.

Key words: mid-infrared laser, LD directly pumping, solid state laser, Ho:BYF laser crystal

LD直接泵浦中红外脉冲固体激光器功率改进研究

张 猛[1], 杨 希[1], 郭嘉伟[1], 蔡 和[1], 吴芯洋[2,1], 韩聚洪[1], 王顺艳[1], 王 滁[1*]

(1. 西南技术物理研究所,四川 成都 610083;
2. 新疆大学 材料科学与工程学院,新疆 乌鲁木齐 830046)

摘要:LD直接泵浦固体激光器具有原理简单、体积小和结构紧凑等优点,该结构用于实现3~5 μm波段的中红外激光输出时具备较大优势。然而,相较于常规近红外LD泵浦的固态激光器,LD直接泵浦中波红外固体激光器存在着较大的量子缺陷,可能导致较大的热损伤并限制其功率的进一步提升。为解决这一问题,本文提出了减小晶体比表面积和改善晶体结构释放热能的方法,并确定了氟化钇钡激光晶体(Ho^{3+}:BY_2F_8)的最佳长度。通过COMSOL软件进行了热力学仿真模拟,研究了不同长度激光晶体的冷却结构。实验结果显示,采用长度略短于冷却器的激光晶体可以提高输出功率并较大缓解激光晶体内部的热应力。实验表明,在泵浦重复频率为15 Hz、脉冲宽度为90 μs,激光器输出波长约为3.9 μm时的单脉冲能量为7.28 mJ,此值长度约为10 mm晶体输出能量(2.81 mJ)的3倍。这一研究结果为未来构建实用化的中波红外激光器铺平了道路。

关 键 词:中波红外激光器;半导体直接泵浦;固体激光器;Ho:BYF激光晶体

中图分类号:TN2 **文献标识码**:A

Received date: 2024-03-13, **revised date**: 2024-04-09 **收稿日期**:2024-03-13,**修回日期**:2024-04-09

Foundation items: Supported by the National Key Research and Development Program of China (2021YFA0718803)

Biography: Zhang Meng (1997-), male, Chengdu, assistant, mainly engaged in the research of beam transmission, laser application and laser processing. E-mail:383919844@qq.com

* **Corresponding author**: E-mail: youwang_2007@aliyun.com

Introduction

The 3-5 μm band radiation is located at the atmospheric infrared transmission window and has ideal air transmission properties. As such a band contains absorption peaks of many molecules, the laser in the mid-infrared band can be widely used in military countermeasures, remote sensing technology, laser surgery, and atmospheric monitoring, etc[1-7]. In some fields, the requirements are often needed on the size, outputted peak power, and repetition rate of a mid-infrared (MIR) laser. Among a variety of conventional solid-state lasers, lamp-pumped solid-state lasers usually have the low pump light-optical conversion efficiency and non-uniform absorption of the laser medium, which lead to the low output beam quality and electro-optical conversion efficiency[6-9]. And at the same time, the output power of a lamp-pumped solid-state laser is not easy to be raised, which is prone to a large amount of energy waste. As most of the output bands of conventional lamp-pumped solid-state lasers are located in the near-infrared region, achieving the output of mid-infrared laser is basically based on the nonlinear optical method such as optical parametric oscillation (OPO) or optical parametric amplification (OPA) methods[10-14]. Although the nonlinear optical procedures have already become mature, the instrumentation is somewhat complex, the number of system components is large, the price is expensive, and the malfunctions are also difficult to avoid. Quantum cascade lasers (QCLs) can also be used for the realization of the mid-infrared laser output. However, it is difficult to build the higher beam quality and high-power laser system at the same time for such semiconductor lasers[15-21]. Being different from the lasers mentioned above, the holmium-doped barium yttrium fluoride laser crystal (Ho^{3+}: BY_2F_8, Ho: BYF) directly-pumped by LDs can be applied to output the mid-infrared laser in which the optical system is simple and the cost of the whole equipment is relatively low[22-28]. However, the quantum defect of the LD directly-pumped laser configuration is much larger than those of conventional near-infrared LD-pumped solid-state lasers. As a result, more heat would be generated during the laser operation. If the heat cannot be quickly dissipated, severe thermal damage may be caused inside the laser medium. In extreme cases, the MIR laser medium may even be broken or blasted[29-33]. This is one of the primary issues that need to be urgently resolved for the development of mid-infrared LD directly-pumped solid-state lasers towards the practicality.

In order to alleviate the problems of thermal deposition of a Ho:BYF crystal and improve the power of a MIR laser, the specific surface area and the structure of the crystals have been theoretically examined in this paper. We refer to the crystal with the length near to the optimal value to obtain the laser output from the theoretical simulation, and propose that the configuration in which the laser crystal is shorter than the cooler might be benefit to enhance the heat dissipation ability of the pumped MIR crystal[29]. And then, two experiments have been conducted to verify the simulation results. In the first experiment, the influence of LD pump sources on the outputted laser power has been investigated by using Crystal-I with the size of 3×3×10 mm. The experimental results show that under the conditions of the repetition rate of 15 Hz, pulse width of 90 μs, and current of 15 A, the single pulse energy of 2.81 mJ can merely be obtained by an energy meter, which corresponds to the average laser output power of 42.15 mW. However, under this pumping condition, the cracks can be observed inside the crystal, which indicates that 2.81 mJ should be near to the limitation that the crystal can critically withstand under such a cooling configuration in the experiment. In the second experiment, results of the simulation and experiment-1 have been well considered by using the optimal crystal length with the size of 3×3×8 mm (Crystal-II). The experimental results show that the pulse energy of 7.28 mJ (corresponding to average laser output power of 109.2 mW) can be achieved under the repetition rate of 15 Hz, the pulse width of 90 μs, and the current of 14.5 A, respectively. As a result, a significant increase in laser outputted power has been successfully achieved. Note that there is no damage in the laser crystal under the improved the lasing structure. These results demonstrate that compared with the traditional method of embedding the laser crystal inside the cooling holder with the same size as the crystal, the structure of the cooler with the length little longer than that of the laser crystal can be really beneficial to improve the heat dissipation ability. The thermal stress of the laser crystal should also be partially relieved by employing this approach. The results reported in this paper is a further breakthrough of our team after we first reported the emission of a mid-infrared Ho:BYF laser directly-pumped by LDs in 2021[29-33]. The study is thought to be helpful for the future practical applications of such MIR solid-state lasers.

1 Theoretical simulation

In this paper, Ho:BYF is used to produce a MIR laser. The energy levels of Ho:BYF are illustrated in Fig. 1. The transition of $^5I_8 \rightarrow {}^5I_5$ represents the process in which the electrons on the ground state energy level is pumped to the upper energy level by using LDs with the wavelength of 889 nm. Then, a 3.9 μm laser is directly generated through the stimulated emission process of $^5I_5 \rightarrow {}^5I_6$. Note that both energy transfer up-conversion (ETU) and cross relaxation (CR) are important processes during the laser emission. The ETU and CR make the MIR lasing very complicated and both of them are all extremely essential for obtaining the MIR oscillation[29-33].

The first LD-directly-pumped solid-state MIR laser has been realized two years before by our laboratory using a 3×3×10 mm Ho:BYF crystal. As the outputted power was far from applications, such a MIR laser cannot be directly applied for any actual purposes. For the improvement of the output power of a Ho:BYF laser, heat accumulation inside the crystal is needed to study. At present, the main methods to alleviate heat accumulation of crystals are reducing the specific surface area of crystals or optimizing the cooling structure. Generally, the heat

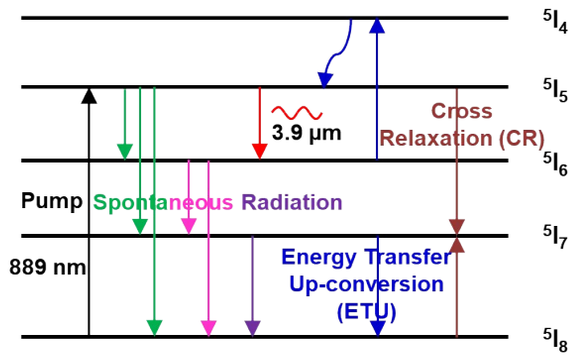

Fig. 1 Energy level diagram of Ho: BYF
图1 Ho:BYF能级示意图

dissipation ability of laser crystals is related to the specific surface area (surface area/volume) presented by the following equation:

$$K = \frac{2a^2 + 4aL_c}{a^2 L_c} = \frac{2}{L_c} + \frac{4}{a} \quad , \quad (1)$$

where K represents the specific surface area value of the crystal, a represents the crystal width, and L_c represents the crystal length, respectively. It is obvious that the shorter the crystal, the larger the specific surface area. Thus, shortening the length of the laser crystal should effectively enhance the heat dissipation ability of the laser crystal and laser output energy under the same pumping conditions.

In addition, the simulation of laser dynamics is also conducted for estimating the outputted pulse energy with different crystal lengths. According to our conclusions in Ref. 29, as shown in Fig. 2, the laser output energy changes with the crystal length. When the pump energy is set between 250 mJ and 350 mJ, the optimal crystal length is around 8 mm.

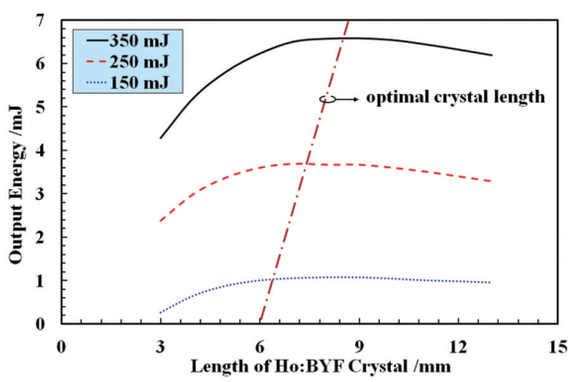

Fig. 2 Theoretical results of the outputted pulse energy versus the crystal length for different pump energy[29]
图2 不同泵浦能量下输出脉冲能量随晶体长度变化的理论结果[29]

Therefore, in order to enhance heat dissipation in crystals, the temperature and thermal stress inside the Ho:BYF medium with two kinds of lengths should be analyzed by using the same cooling configuration, as shown in Fig. 3. The corresponding thermal simulation of heat dissipation in crystals was carried out in detail for Crystal-I and Crystal-II by utilizing COMSOL. Figures 4 and 5 show the temperature at Point A in Fig. 3 and thermal stress inside Crystal-I (3×3×10 mm) and Crystal-II (3×3×8 mm) under the same pumping conditions, respectively. The boundary conditions for COMSOL thermal simulation are listed in Table 1. From Fig. 4, although Crystal-II produces a little more temperature raising, which is also due to its smaller volume than that of Crystal-I, the minimum temperature of two crystals is almost the same before the next pump pulse reaches the crystal. Such phenomenon indicates that changing the pump length should be conducive to the heat dissipation of the crystal. As shown in Fig. 5, the thermal stress of Crystal-II is less than that of Crystal-I for the improved cooling structure. This means that it should be beneficial to alleviate the thermal stress of the crystal by adopting such a shorter crystal.

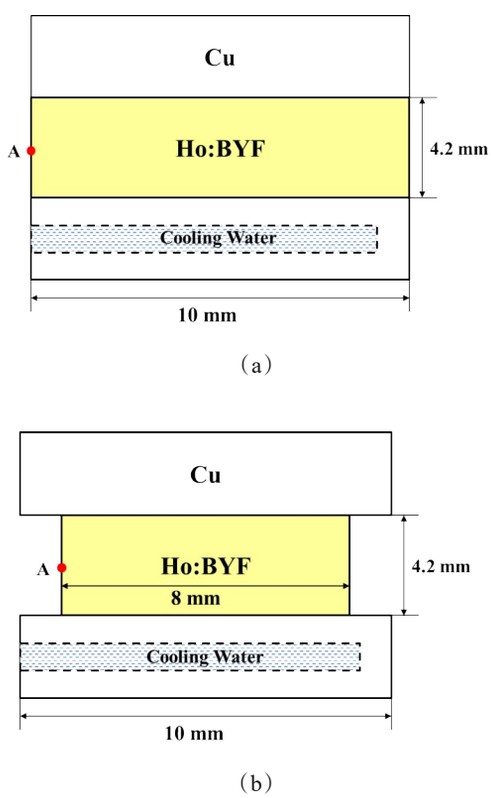

Fig. 3 Cooling structures: (a) crystal-I; (b) crystal-II
图3 冷却结构: (a)晶体-1;(b)晶体-2

In order to verify the theoretical simulation results, two experiments have been carried out for the laser media with different lengths. Therefore, the influence of the pulse width, driving current, and repetition rate of the pump LDs on the outputted laser energy has been experimentally explored by using such two Ho: BYF crystals. The results will be inducted in Sections 3 and 4.

Table 1 Boundary conditions of thermal simulation
表 1 热模拟的边界条件

Parameters	Values and units
Peak power	2860 W
Pulse width	90 μs
Pulse frequency	15 Hz
Beam diameter	1. 2 mm
Air temperature	27 ℃
Cooling temperature	27 ℃

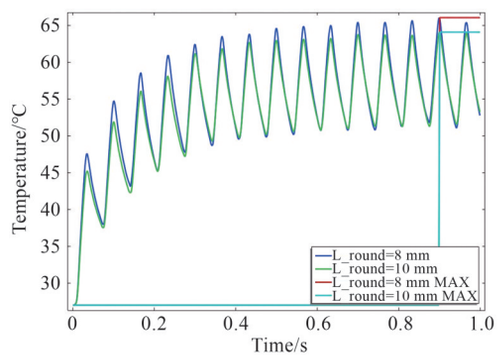

Fig. 4 Theoretical results of the temperature variation of two crystals under the same pumping condition
图4 两种晶体在相同泵浦条件下温度变化的理论结果

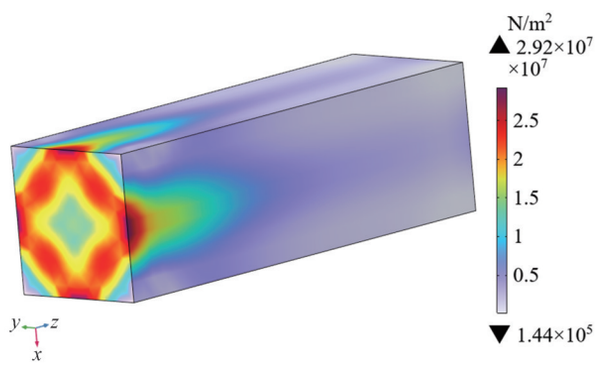

(a)

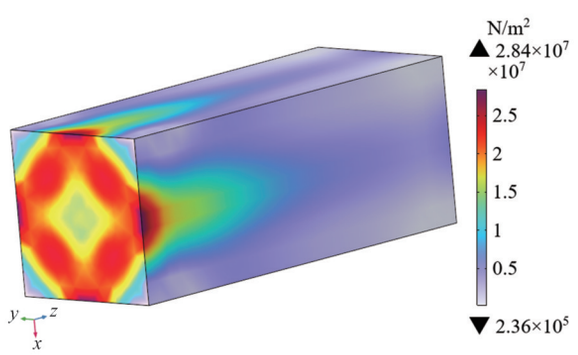

(b)

Fig. 5 Simulated thermal stress of (a) crystal-I; (b) crystal-II under the same pumping conditions
图5 相同泵浦条件下的模拟热应力:(a) 晶体I;(b) 晶体II

2 Experiment-1: investigation of the damage threshold of pump LDs for Crystal-I

Figure 6 shows the clamping diagram and section diagram of C-C′ plane for Crystal-I. The Ho:BYF crystal was fixed in a rhombus-shaped holder combined by the upper and lower parts. The indium foil was intentionally paved between the brass seat and the crystal to fill the gaps as much as possible.

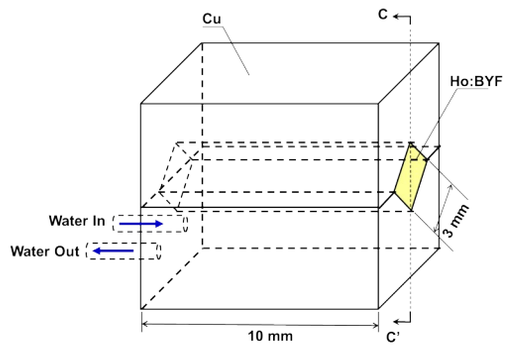

(a)

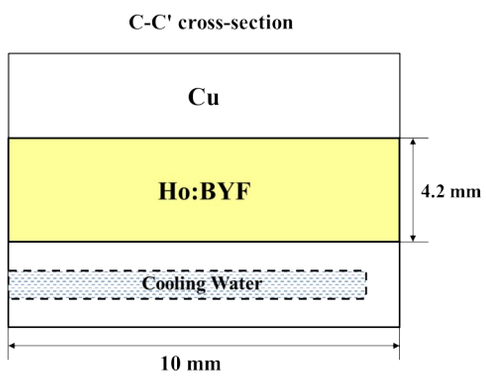

(b)

Fig. 6 (a) Clamping diagram; (b) section diagram of the C-C' plane for crystal-I
图6 晶体-I的(a)夹具图和(b) C-C′面截面图

The schematic diagram and the photograph of our experimental setup are shown in Figs. 7 and 8, respectively. The light of pump LDs with the central wavelength of 889 nm was changed into a parallel beam by using the first plano-convex focus lens with the focal length of 75 mm. Then the paralleled LD radiation was focused by the second plano-convex focus lens (f = 75 mm). The converge pump beam with the diameter of 650 μm enters into a plano-concave optical resonator consisting of a rear mirror (RM), an output mirror (OC), and Ho:BYF gain medium, Crystal-I. And then, a MIR laser with the wavelength of 3. 9 μm can be directly obtained[29]. In the experiments, a He-Ne laser was used to calibrate the op-

tical path of the oscillator and a silicon wafer was used to filter out the components of the pump light mixed in the output beam. Actually, the measured output values are about a half of the real results because of the attenuation of such a silicon wafer.

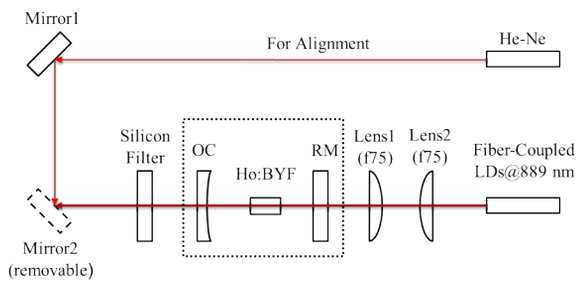

Fig. 7 Schematic illustration of the experimental setup
图7 实验装置示意图

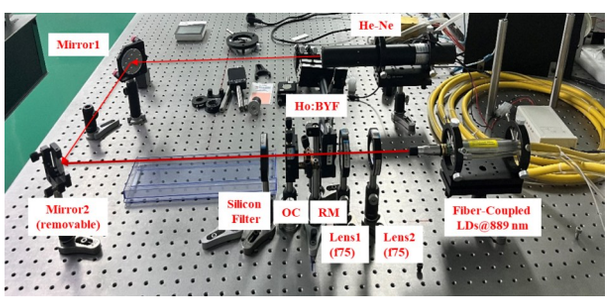

Fig. 8 Photograph of our experimental system
图8 我们的实验观光路图

In this experiment, the repetition rate of the pump laser was first set to 2 Hz, and the driving current of the pump LDs was set to 14 A, 16 A, and 18 A, respectively. When the pulse width of the pump laser was changed from 60 μs to 130 μs, the laser output energy was observed by means of an energy meter.

Fig. 9 shows the experimental results. It can be seen that the output energy of the MIR laser increases with the pump pulse width roughly acting as multiple curves. Under the same pulse width, the laser output energy increases with the driving current of the pump. With the increase of the pump driving current, the laser output energy changes smoother. The laser output energy can reach up to 12 mJ when the pump driving current and pulse width are set to 18 A and 120 μs, respectively.

Then, as shown in Fig. 10, the relationship between the driving current of the pump LDs and the laser output energy under the repetition rate of the pump LDs of 2 Hz was investigated using the pump pulse width of 60 μs, 80 μs, 100 μs, and 120 μs, respectively. It can be seen that the laser output energy increases with the driving current of the pump LDs. And the curves somewhat appear to be linear forms within a certain range, which indicates that the influence of the pump pulse width on the laser output energy is slightly stronger than that of the pump driving current. The variation of the laser output energy becomes more drastic for a wider pump pulse width.

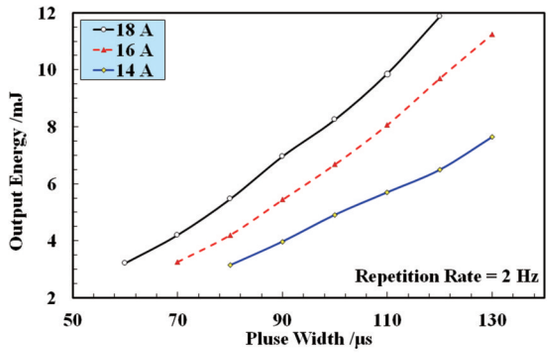

Fig. 9 Relationship between the pump pulse width and the laser output energy (Repetition Rate = 2 Hz)
图9 泵浦脉宽与激光输出能量的关系(重复频率为2 Hz)

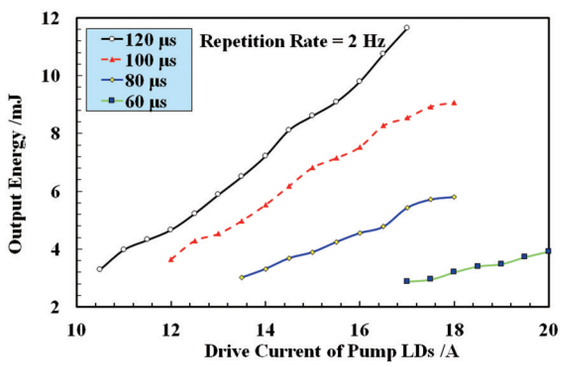

Fig. 10 Relationship between the drive current of pump LDs and the laser output energy (Repetition Rate = 2 Hz)
图10 泵浦LD驱动电流与激光输出能量的关系(重复频率为2 Hz)

Next, the laser output energy was examined for different pump repetition rates when the pulse width of the pump was set to 90 μs, and the driving current of the pump LDs were set to 14 A and 15 A, respectively. As can be seen from Fig. 11, the laser output energy decreases with the pump repetition rate, and the corresponding energy of the pulse laser decreases, but the average output power of the MIR laser shows an increasing trend. The laser output energy increases with the pump energy under the same repetition rate. When the repetitive rate, the pulse width, and the drive current is 90 μs, 15 Hz, and 15 A, respectively, the pulse energy can be obtained as about 2.81 mJ, which is converted to an average laser output power of 42.15 mW. After several ten seconds under such conditions, the crystal was suddenly destroyed and a deep crack was found at the input end of the crystal, which indicates that all the parameters here should correspond to the destroy threshold conditions that the laser crystal can withstand. Note that the pumping energy is approximately 221.8 mJ at that time.

Combined with the results of the above experi-

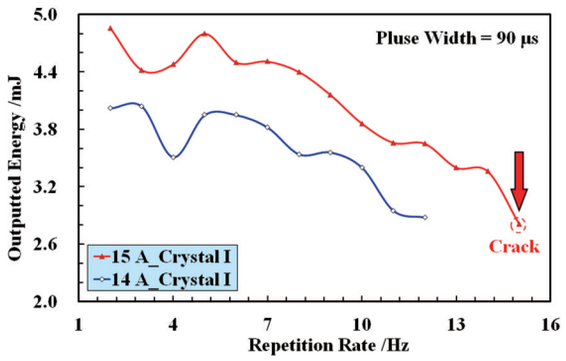

Fig. 11 Relationship between the pump light repetition rate and the laser output energy (Pulse Width = 90 μs)
图 11 泵浦光重复率与激光输出能量的关系(脉冲宽度为 90 μs)

ments, it has been analyzed that the pump pulse width and pump LD drive current have less influence on the laser output energy than the pump repetition rate. Therefore, in the following experiments, the values of pump pulse width and pump LD drive current were fixed, and the pump repetition rate was taken as a variable factor.

3 Experiment-2: improvement of laser output for Crystal-II

Figure 12 shows the schematic clamping diagram and the section diagram of the C-C′ plane of Crystal-II by employing the same cooling configuration as that for Crystal-I.

In order to obtain the high outputted laser energy without damaging the crystal, the pump pulse width at 90 μs, and the pump LD drive current at 14 A and 14.5 A were set as safe values, and the repetition rate of the pump laser was changed to observe the change of the outputted laser energy.

Figure 13 shows the energy and power diagrams of the laser output. From Fig. 13, we can see that the laser output energy still shows a decreasing trend with the pump repetition rate, while the overall output power of the laser still shows an increasing trend. In the case of the pump repetition rate of 15 Hz, the pulse width of 90 μs, the current of 14.5 A, the pulse energy can be measured by an energy meter as 3.64 mJ. Taking into account that such value is the result attenuated by the silicon wafer, and the actual laser output energy is exactly twice as much as the measured value, so the actual output energy of the MIR laser is 7.28 mJ (corresponding laser output average power of 109.2 mW). Note that, there is no cracks in the crystal at that time.

It can be seen that, when using a new shorter laser crystal, the MIR laser output energy has been greatly improved. The structure that the length of the laser crystal is slightly shorter than the cooler has been proved to significantly improve the heat dissipation capacity of the laser crystal. Therefore, further optimization on the pump structure and the shape of a laser crystal should be the important way to achieve much higher outputted power of our MIR laser in the future.

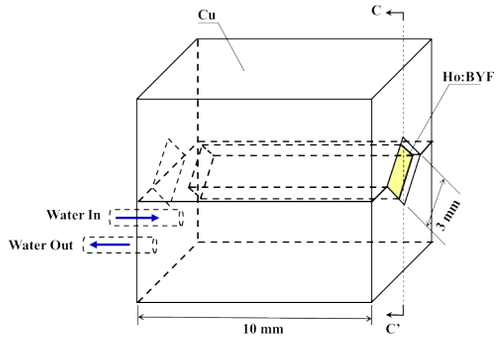

(a)

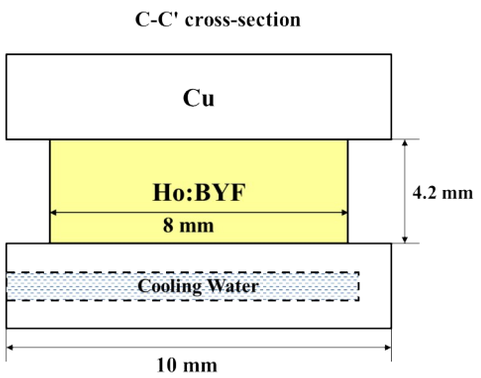

(b)

Fig. 12 (a) Schematic of clamping diagram and (b) section diagram of the C-C' plane for crystal-II
图 12 (a) 晶体-II的夹具示意图和(b) C-C′面剖面图

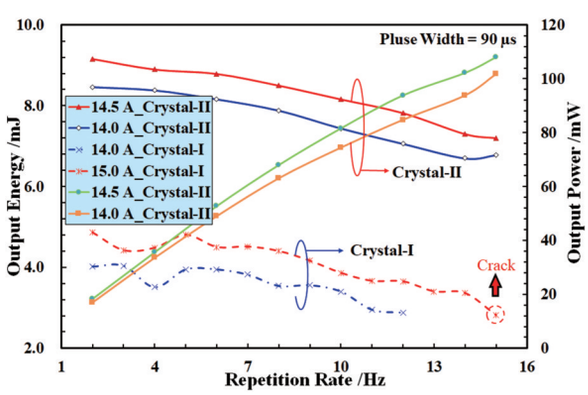

Fig. 13 Relationship between the repetition rate and the laser output energy and power for both crystal-I and crystal-II (Pulse Width = 90 μs)
图 13 在脉冲宽度为 90 μs时,晶体 I 和晶体 II 的重复频率与激光输出能量的关系

4 Conclusions

In this paper, the length of a MIR medium, Ho: BYF, has been analyzed to earn the output energy as large as possible based on the theoretical simulations of laser dynamics. The theoretical computation of thermal

dynamic reveals that the suitable length of a Ho:BYF crystal makes the output of a MIR laser be substantially enhanced and the heat dissipation ability significantly improve inside the laser crystal. The experimental results show that with the pump repetition rate of 15 Hz, the pulse width of 90 μs, and the drive current of 14.5 A, the pulse energy of the laser can achieve 7.28 mJ for a Ho:BYF crystal with the length near to the optimal value in theory. Such result is about four times as large as that in Ref. 29 for LD directly-pumped MIR lasers. Our work might lay the technical foundation for the realization of practical MIR solid-state lasers directly-pumped by LDs.

References

[1] Werle P, Slemr F, Maurer K, *et al*. Near- and mid-infrared laser-optical sensors for gas analysis[J]. *Optics and Lasers in Engineering*, 2002, **37**(2/3):101-114.

[2] Tittel F K, Richter D, Fried A. Mid-infrared laser applications in spectroscopy[J]. *Springer Berlin Heidelberg*, 2003, 458-529.

[3] Willer U, Saraji M, Khorsandi A, *et al*. Near- and mid-infrared laser monitoring of industrial processes, environment and security applications [J]. *Optics & Lasers in Engineering*, 2006, **44**(7): 699-710.

[4] Barnes, Norman P, Walsh, *et al*. Mid infrared lasers for remote sensing applications[J]. *Journal of Luminescence*, 2016, **169**: 400-405.

[5] Wang Z, Zhang B, Liu J, *et al*. Recent developments in mid-infrared fiber lasers: Status and challenges[J]. *Optics & Laser Technology*, 2020, **132**:106497.

[6] Li X, Huang X, Hu X, *et al*. Recent progress on mid-infrared pulsed fiber lasers and the applications[J]. *Optics & Laser Technology*, 2023, **158**: 108898.

[7] Henderson-Sapair O, Munch J, David J, *et al*. Mid-infrared fiber lasers at and beyond 3.5 μm using dual-wavelength pumping[J]. *Optics letters*, 2014, **39**(3):493-496.

[8] Sorokin E, Naumov S, Sorokina I T. Ultrabroadband infrared solid-state lasers[J]. *IEEE Journal of Selected Topics in Quantum Electronics*, 2005, **11**(3): 690-712.

[9] Rudy C W. Mid-IR lasers: Power and pulse capability ramp up for mid-IR lasers[J]. *Laser focus world*, 2014, **50**(5): 63-66.

[10] Ren T, Wu C, Yu Y, *et al*. Development progress of 3-5 μm mid-infrared lasers: OPO, solid-state and fiber laser[J]. *Applied Sciences*, 2021, **11**(23):11451.

[11] Baumgartner R A, Byer R L. Optical parametric amplification[J]. *IEEE Journal of Quantum Electronics*, 1979, **15**(6):432-444.

[12] Wang P, Shang Y, Li X, *et al*. Multi-wavelength mid-infrared laser generation based on optical parametric oscillation and intracavity difference frequency generation[J]. *IEEE Photonics Journal*, 2016, **9**(1): 1-7.

[13] Li C, Xie J J, Pan Q K, *et al*. Progress of mid-infrared optical parametric oscillator[J]. *Chinese Optics*, 2016, **9**(06): 615-624.

[14] Chen B Y, Wu S, Yu Y J, *et al*. 3.8 μm mid-infrared optical parametric amplifier based on MgO:PPLN crystal-ScienceDirect[J]. *Infrared Physics & Technology*, 2020, **111**: 103448.

[15] Kolhed M, Haberkorn M, Pustogov V, *et al*. Assessment of quantum cascade lasers as mid infrared light sources for measurement of aqueous samples[J]. *Vibrational spectroscopy*, 2002, **29**(1-2): 283-289.

[16] Hvozdara L, Pennington N, Kraft M, *et al*. Quantum cascade lasers for mid-infrared spectroscopy[J]. *Vibrational Spectroscopy*, 2002, **30**(1):53-58.

[17] Yao Y, Hoffman A J, Gmachl C F. Mid-infrared quantum cascade lasers[J]. *Nature Photonics*, 2012, **6**(7):432-439.

[18] Razeghi M, Bandyopadhyay N, Bai Y, *et al*. Recent advances in mid infrared (3-5 m) quantum cascade lasers[J]. *Optical Materials Express*, 2013, **3**(11):1872-1884.

[19] Isensee K, Kroger-Lui N, Petrich W. Biomedical applications of mid-infrared quantum cascade lasers-a review[J]. *Analyst*, 2018, **143**(24): 5888-5911.

[20] Ma Y, Ding K, Wei L, *et al*. Research on mid-infrared external cavity quantum cascade lasers and applications[J]. *Crystals*, 2022, **12**(11): 1564.

[21] Slivken S, Razeghi M. High power mid-infrared quantum cascade lasers grown on GaAs[C]. Photonics. MDPI, 2022, **9**(4): 231.

[22] Hoffman H, Jennsen H. Multi-wavelength, efficient mid-infrared laser system[J]. 1998.

[23] Tabirian A M, Jenssen H P, Cassanho A. Efficient, room temperature mid-infrared laser at 3.9 μm in Ho: BaY_2F_8[C]. Advanced Solid State Lasers. Optica Publishing Group, 2001: MC5.

[24] Stutz R, Miller H C, Dinndorf K M, *et al*. High-pulse-energy 3.9-μm lasers in Ho: BYF[C]. Solid State Lasers XIII: Technology and Devices. SPIE, 2004, **5332**: 111-119.

[25] Han L, Zou Y, Liu J, *et al*. Effect of intrinsic point defects on the electronic and optical properties of Ho: BYF crystal[J]. *Optical Materials*, 2021, **121**: 111514.

[26] Liu J, Zhang T, Jia B, *et al*. Electronic and optical properties of Ho-doped BYF crystal [J]. *Chinese Journal of Physics*, 2020, **65**: 604-612.

[27] Zeng F M, Zou G T, Liu J H. Growth and absorption spectrum of Tm, Ho: BaY_2F_8 crystal[J]. *Advanced Materials Research*, 2011, **335**: 1025-1028.

[28] Ji E C, Liu Q, Nie M M, *et al*. Spectroscopic properties of heavily Ho^{3+}-doped barium yttrium fluoride crystals[J]. *Chinese Physics B*, 2015, **24**(9): 094216.

[29] Zhang Y, Ma C Q, Guo J W, *et al*. Theoretical analyses and configuration optimizations of a LD-pumped 3.9 μm Ho: BYF laser[J]. *Optics & Laser Technology*, 2022, **148**: 107769.

[30] Ma C Q, Zhang Y, Cai H, *et al*. A 3.9 μm Ho3+: BYF laser pumped by a three-mirror cavity Cr: LiSAF laser with high optical-to-optical efficiency [C]. AOPC 2021: Infrared Device and Infrared Technology. SPIE, 2021, 12061: 455-462.

[31] Ma C Q, Zhang Y, Guo J W, *et al*. A 3.9 μm Ho^{3+}: BaY_2F_8 laser directly pumped by laser diodes [J]. *Electronics Letters*, 2021, **57**(20): 779-781.

[32] Rong K P, Cai H, Liu X X, *et al*. : Theoretical evaluation of a pulsed mid-infrared Ho3+: BaY2F8 laser [C]. 2019 IEEE 4th Optoelectronics Global Conference (OGC), Shenzhen, 2019,76-80.

[33] Rong K P, Wang Y, Yu H, *et al*. Theoretical evaluation of a continues-wave Ho^{3}+: BaY_2F_8 laser with mid-infrared emission[C]//2017 International Conference on Optical Instruments and Technology: Advanced Laser Technology and Applications. SPIE, 2018, **10619**: 22-30.